Antarctic Science 12 (1): 119–124 (2000) © British Antarctic Survey Printed in the United Kingdom

The effect of ocean tidal loading on satellite altimetry over Antarctica

DONGHUI YI[1,2], J. BERNARD MINSTER[2]* and CHARLES R. BENTLEY[1]

[1]*Geophysical and Polar Research Center, University of Wisconsin at Madison, Madison, WI 53706, USA*
[2]*IGPP, Scripps Institution of Oceanography, University of California at San Diego, La Jolla, CA 92093, USA*
**Corresponding author*

Abstract: Vertical displacements of emerged land caused by oceanic tidal loading are of the order of several tens of millimetres in polar regions. They constitute a long wavelength signal, the amplitude of which is comparable to elevation changes that might be associated with climate-driven changes in ice-sheet volume. Using bilinear interpolation on a 1° by 1° global grid, we examine the amplitudes and phases of vertical displacements caused at any given epoch by the eight most important ocean tide constituents of recent ocean tide models, extrapolated to high latitudes. This permits estimation of the oceanic tidal loading corrections to measurements made by a satellite altimeter along the satellite ground track. We have done so systematically over Antarctica, for a scenario flight of ICESAT, which carries the Geoscience Laser Altimeter System (GLAS), whose primary science goal is to monitor ice-sheet mass balance. Ocean loading tide corrections near the coast of Antarctica can reach several centimetres; overall they average about 10 mm.

Received 18 December 1998, accepted 27 November 1999

Key words: ice sheet, mass balance, remote sensing

Introduction

If melted, Antarctic ice would produce *c.* 65 m rise in sea level (Oerlemans 1993). For this reason alone, we need to understand how the Antarctic ice sheet will respond to current climate change. In the present century, sea level has risen at a rate of 1.0–2.0 mm yr^{-1} (Warrick 1993). Part of it can be explained by thermal expansion of the ocean water and melting of glaciers, small ice caps, and, perhaps, the Greenland ice sheet. For comparison, the annual snowfall on the grounded Antarctic ice is equivalent to about 5 mm yr^{-1} of global sea-level change (Jacobs 1992), so interannual variations in Antarctic snow accumulation rates alone are a source of measurable sea level fluctuations. Similarly, should half of the rate in sea-level rise, i.e. 0.5–1.0 mm yr^{-1}, be balanced by a secular change in the volume of the Antarctic ice sheet, then the mean surface elevation of the ice should be observed to drop at a rate of about 15–30 mm yr^{-1}. This shows that, without much better knowledge of the contributions of the Antarctic ice sheet, our understanding of sea-level change will remain plagued by major uncertainty (Warrick & Oerlemans 1990).

Satellite altimeters offer great promise for monitoring the volume of the polar ice sheets. Considerable progress in polar mass-balance study has accrued from the use of radar altimeters such as Seasat, Geosat, and ERS1/2 (Brenner *et al.* 1983, Zwally *et al.* 1989, Zwally 1989, Partington *et al.* 1991, Bentley & Sheehan 1992, Lingle *et al.* 1994, Yi *et al.* 1997). However, the precision of radar altimeters is limited by surface slope, because of their large kilometre-size footprints (Brenner *et al* 1983), by the microwave penetration into the subsnow surface (Ridley & Partington 1988, Yi & Bentley 1997), and by the imprecision of the satellite orbits (Haines *et al.* 1994). In contrast, the primary science goal of the Geoscience Laser Altimeter System (GLAS) (2001 launch, Schutz 1995) will be to measure volume changes in the polar ice sheets. This instrument offers a much smaller (70 m) footprint that will reduce the surface–slope effect and an on-board GPS receiver that will ensure an orbit accuracy of ± 50 mm both along and across-track.

Both ocean tides and solid-earth tides have been taken into account in processing satellite radar altimetry data (e.g. Zwally *et al.* 1990), but the smaller vertical deflection of the land surface caused by oceanic tidal loading has not been given detailed attention. This is not surprising, since this displacement is only of the order of tens of millimetres even along the coast, a small correction compared to the precision of radar altimeters over land (tens of centimetres). Ocean loading effects will become important, however, when surface elevation measurements reach centimetre-level precision, as is the case for GLAS. To determine surface elevations and their temporal changes accurately, spatial and temporal variations of oceanic tidal loading and its effects on altimetry measurements are essential.

Ocean tidal loading

Various methods have been used to compute tidal loading. Baker (1985) lists five of them: (1) the spherical harmonic expansion method; (2) the polygon method; (3) the template method; (4) the spherical disc method; and (5) the Green's function method. In this study, we use the Green's function

https://doi.org/10.1017/S0954102000000158 Published online by Cambridge University Press

method (Farrell 1972). Agnew (1996) developed convenient and widely used software to calculate the load tide time series at a given location, using a Green's function and an ocean tide model. He represents the ocean load tide L by

$$L(\theta',\lambda') = \int_0^{2\pi}\left(\int_0^{\pi}\rho H(\theta,\lambda)G_L(\Delta)S_L(\alpha)a^2\sin(\theta)d\theta\right)d\lambda, \quad (1)$$

where Δ is the distance; α is the azimuth of the point with geographical coordinates (θ,λ) relative to the point of observation (θ',λ'), H is the tidal height at (θ,λ), ρ the density of ocean water, and a the radius of the earth. In Eq. 1, G_L is the Green's function appropriate for mass-loading (taken from Farrell 1972), and S_L is the combination of trigonometric functions that arises when computing a vector or tensor load. Many global tidal models are available for ocean tide loading calculations, starting with the Schwiderski model (Schwiderski 1980). More recent models such as the CSR 3.0 model (Eanes 1994), the TPXO.2 model (Egbert *et al.* 1994), and the FES95.2 model (Le Provost *et al.* 1994, 1995) have been improved considerably as a result of altimetry missions, particularly TOPEX-Poseidon. Following the treatment described in the International Earth Rotation Service (IERS) standards (McCarthy 1992) the displacement component at a particular location is represented by

$$\Delta C = \sum_j f_j A_j \cos(\omega_j t + \chi_j + \mu_j - \Phi_j), \quad (2)$$

where the index j refers to a particular tidal constituent; f_j and μ_j depend on the longitude of the lunar node (Doodson 1928); A_j, Φ_j and ω_j are the amplitude (from Eq. 1), phase, and angular frequency of that constituent, respectively; and χ_j is the astronomical argument at t = 0. All three components of displacement (vertical, east–west, north–south) can be calculated using these equations; but this study considers only the vertical component.

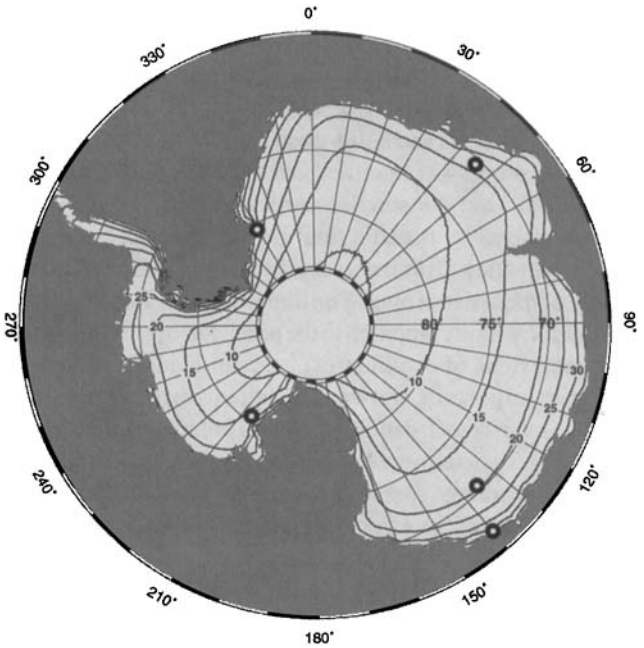


Fig. 1. Upper bound on the amplitudes of vertical displacements due to ocean tide loading in Antarctica, obtained by summing the amplitudes calculated for eight tidal constituents, namely M_2, N_2, S_2, K_2, K_1, O_1, Q_1 (from ocean tide model FES95.2) and P_1 (from model TPXO.2). The five circles denote locations used to test the accuracy of the interpolation procedure.

Results and discussion

Equation 2 was evaluated for the eight major tidal constituents (four semidiurnal waves M_2, N_2, S_2, K_2, and four diurnal waves K_1, O_1, P_1, Q_1) that contribute the most to tidal loading. The tidal model FES95.2 was used to calculate the amplitude and phase of all constituents except P_1, which is not contained in FES95.2 and for which model TPXO.2 was used. We selected FES95.2 mainly because it is the only global ocean tide model that includes at least some data from the regions under the Ross and Filchner–Ronne ice shelves in Antarctica.

For verification, the vertical displacement computed here was compared with results that use the same amplitude and phase calculations as McCarthy's (1992). McCarthy's method was described by Scherneck (1991). At a test point (66.6617°S, 140.0014°E) in Antarctica, for a 180-day period starting 1 January 2001, the differences between the two calculations do not exceed ± 1.6 mm. McCarthy's results are thought to be accurate to ± 3 mm (McCarthy 1992). Since we are using a more recent, improved tide model, it is reasonable to assume that the accuracy of our calculations is at least as good.

The calculated vertical tidal-loading displacements are typically a few centimetres over Antarctica; they are lower inland and higher in coastal regions, as expected. An upper bound on the total tidal displacement may be estimated by taking all constituents to be in phase, and summing their amplitudes. Figure 1 shows the distribution of

$$A = \sum_{j=1}^{8} A_j$$

which ranges up to 65 mm (130 mm peak to peak). However, taking phase relationships into account, the elevation fluctuations are substantially smaller. For example, at (66°S, 100°E), A ≈ 40 mm (80 mm peak to peak), but the peak to peak range of the displacement time series reaches only about 60 mm in the first ten years of the 21st century. Of course, the upper bound always will give an over-estimate of the maximum possible amplitude. For example, when M_2, S_2, and K_2 coincide in phase at an equinoctial spring tide, the diurnal components cancel each other in phase and amplitude. Similarly, when O_1, P_1, and K_1 coincide in phase at solstitial spring tide, K_2 is in opposition to S_2 (D.E. Cartwright, personal communication 1999).

Since the load tide varies smoothly, both spatially and temporally, it can be interpolated in space and time with negligible error, as illustrated in Figs 2 (time interpolation)

https://doi.org/10.1017/S0954102000000158 Published online by Cambridge University Press

and 3 (space interpolation). In Fig. 2 there are actually two time series plotted, one calculated every 0.2 hours and one calculated at hourly intervals and linearly interpolated every 0.2 hr; the two are indistinguishable. Similarly, in Fig. 3, two estimates of load tides are compared at constant (70°S) latitude, and half-degree intervals in longitude. In one case, the calculation is performed for each longitude sample and, in the other, the calculation is only performed at integral longitudes and interpolated at the half-degree points. Again, the difference is negligible, justifing our approach of tabulating load tide amplitudes and phases on a 1° x 1° geographical grid. To estimate tidal-loading displacements at any given time and any given point we use bilinear interpolation (e.g. Press *et al.* 1992) to compute the appropriate amplitude and phase at that location, and use Eq. 2. As a check, we compared calculated and interpolated values for a 180-day time series sampled at hourly intervals, starting 1 January 2001, at five locations within the continent. The first point (66.6617°S, 140.0014°E), is near the east Antarctic coast; the second (70.5°S, 135.5°E), and third (70.5°S, 45.5°E) points are inland; the fourth point (80.5°S, 30.5°W) is near the Filchner Ice Shelf; and the fifth one (80.5°S, 144.5°W) is near the Ross Ice Shelf. The standard deviations of the residuals between calculated and interpolated values are 0.35 mm, 0.05 mm, 0.03 mm, 0.85 mm, and 0.11 mm, respectively. These values lie well within the accuracy requirements for GLAS. In view of the results shown in Figs 2 & 3, it is clear that calculation of the tides at grid nodes need only be performed once during the time taken by the ICESAT spacecraft to traverse any given grid cell. This suggests that an effective strategy for GLAS would be to compute the corrections at only a relatively sparse set of points – say, every 15 seconds, i.e. every 600 laser shots, or every degree along track – and to interpolate using the shot count as the independent variable along track.

A typical technique used to process satellite altimeter data is "crossover analysis," in which measurements made along ascending and descending ground tracks crossing over a common surface point are compared. For this study, the positions of Antarctic crossover points and the overflight times along the ascending and descending passes over those points for a scenario GLAS mission were provided by B.E. Schutz (personal communication 1997). These points are computed for a 94° inclination orbit at altitude 705 km, with a hypothetical launch time of 01-01-2001, 00:00 GMT. The various panels in Fig. 4 summarize several aspects of the tidal-loading terms for a crossover point at (67.7799°S, 101.9368°E) for the year 2001. Figure 4a shows the tidal loading displacements at hourly intervals through the year. The histogram of these displacement values, shown in Fig. 4b shows that the distribution is significantly skewed at that location, although the mean over the 365-day cycle is very close to zero. This skewness is caused primarily by the near-commensurability (exact in the case of K_1 and K_2) of the frequencies of certain tide components. (For instance, the histogram of values of the function $\cos \omega t + \cos 2\omega t$ is skewed, extending from a minimum of -1.2 to a maximum value of +2.) Furthermore, because this commensurability is exact by definition for components K_1 and K_2, this phenomenon will persist forever. It should be noted that the degree of skewness is a function of time, and since it depends on the relative phases of the components, it depends also on location. If the beat period is in turn comparable to the repeat period of the sampling by GLAS, then it is possible for tidal loading signals to appear as small, but geographically coherent, long-term apparent changes in the average distribution of ice across the

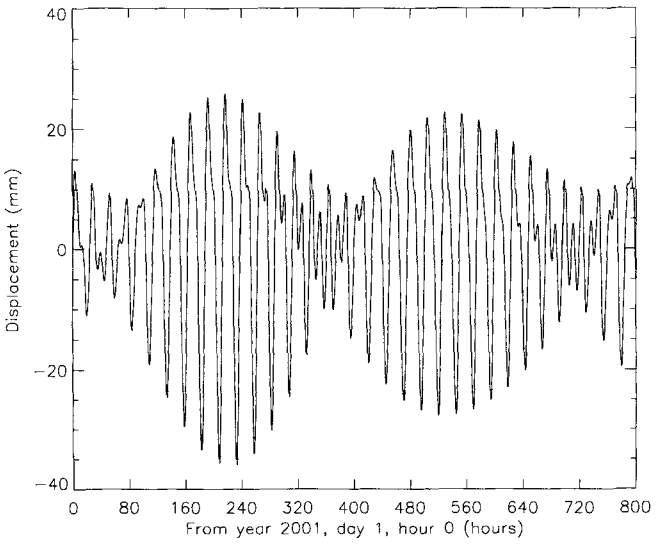


Fig. 2. Vertical displacements calculated at (66.0°S, 120.0°E) at 1-hour and 0.2-hour intervals, respectively. The two curves are indistinguishable.

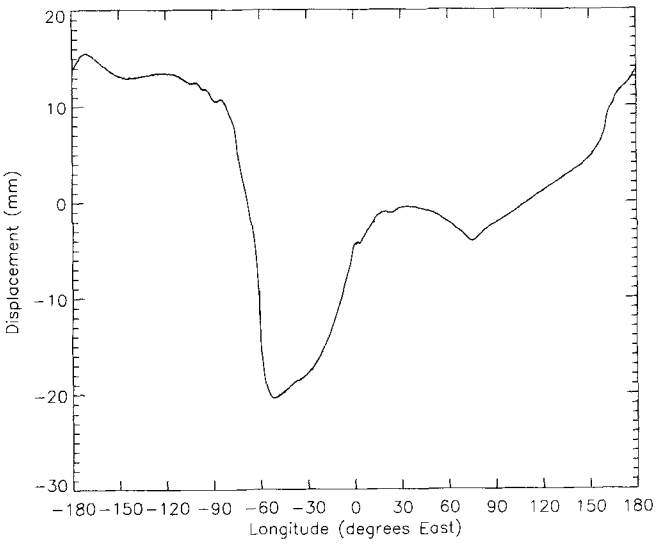


Fig. 3. Vertical displacements at epoch 2001 00:00:00, along a small circle of latitude 70°S. Two estimates are shown, calculated at points separated by 1° and 0.5° longitude intervals, respectively. The two curves are indistinguishable.

https://doi.org/10.1017/S0954102000000158 Published online by Cambridge University Press

Table I. Tide frequencies and vertical displacement at location 67.7799°S, 101.9368°E.

Tide	Frequency (Degree/hour)	Vertical Displacement (mm)
M_2	28.9841	4.7
N_2	28.4397	1.4
S_2	30.0000	2.0
K_2	30.0821	0.8
K_1	15.0411	7.9
O_1	13.9430	7.2
P_1	14.9589	2.4
Q_1	13.3987	1.4

ice sheet. It is therefore important to perform this correction as accurately as possible. Table I shows the frequencies and amplitudes of the tides summed at the test point, and Table II

Table II. Beat periods of selected pairs of tidal components.

Tide Pairs	Beat Period (yrs)
$K_1 \sim K_2$	∞
$K_2 \sim S_2$	0.50
$P_1 \sim S_2$	0.50
$P_1 \sim K_2$	0.25

shows long beat periods generated by four tide pairs. The actual skewness and its actual geographical distribution is, of course, a result of the complex pattern of relative phases of all these components.

How the time series shown in Fig. 4a is actually sampled by ascending and descending passes in an 8-day-repeat orbit is illustrated in Figs 4c & e, and the corresponding histograms are shown in Figs 4d & f, respectively. In both cases, a clear

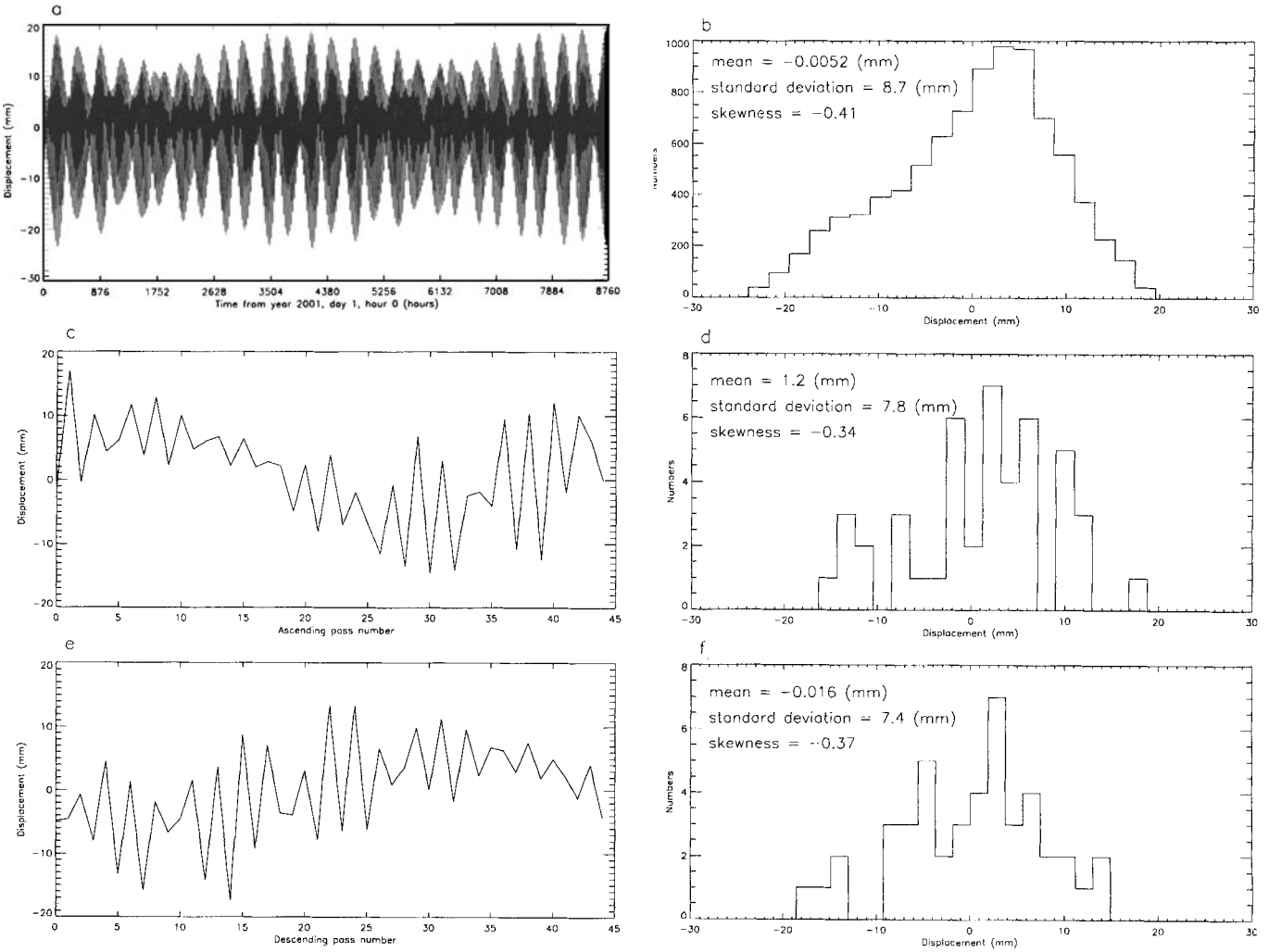


Fig. 4. Vertical-displacement time series and associated histograms at 67.7799°S, 101.9368°E. **a. & b.** show the complete time series and related histogram calculated at 1-hr intervals. **c. & d.** show how this time series would actually be sampled in an 8-day-repeat GLAS mission scenario for calendar year 2001 (94° inclination, 705km orbit, 2001 00:00:00 launch) by ascending passes only; and **e. & f.** show the sampling by descending passes. (An 8-day-repeat cycle yields 45–46 ascending and descending passes each over a particular location on the surface.)

https://doi.org/10.1017/S0954102000000158 Published online by Cambridge University Press

quasi-seasonal signature emerges, which is quite different for ascending and descending passes. This is due to the beat pattern that arises between the various orbital periodicities and quasi-periodicities and the periods of the various tidal constituents, so that this pattern is clearly expected to depend on the specific mission scenario used in the calculation. The pattern will not be exactly seasonal and will be different for different orbits (Parke *et al.* 1987). Note that the histograms for the entire 365-day cycle retain a near-zero mean, and a variance comparable to the original time series, for both the ascending and descending sets of passes. Nearly contemporary ascending and descending passes can yield values that differ by as much as 35 mm whilst subsets of passes selected to seek seasonal variability in the surface elevations can show a systematic bias in either direction. This means in turn that it is possible, given certain combinations of mission scenarios and data subsets, that uncorrected load tide effects might masquerade as measurable secular elevation changes.

Since the load tide signals are controlled both by the ocean tide distribution and the geometry of the continent-ocean boundary, they should exhibit a strong geographical dependence. For example, the longitudinal variation of the RMS displacements is illustrated in Fig. 5 for three different latitudes. These RMS values were calculated for the first 45 sets of ascending and descending passes, starting on 1 January 2001. They highlight the signatures around the Ross Sea (near longitude 190°) and the Weddell Sea (near longitude 310°), and show clearly how the load tide amplitudes decrease inland, away from the shoreline. In Fig. 6 the RMS values of vertical displacements calculated at hourly intervals for the entire year 2001 have been contoured over the relevant portion of Antarctica. The circular area surrounding the pole at latitudes above 86° is not sampled by the 94° inclination orbit in this GLAS mission scenario. Not surprisingly, the pattern that emerges in Fig. 6 is quite similar to that of the "maximum possible" displacements shown in Fig. 1, although the amplitudes are smaller by a factor of 2 to 3.

We should note that the largest amplitudes, seen along the coast lines and emphasized near the extensive, shallow ocean overlying the continental shelves of the Ross and Weddell seas and their extensions southward between the Ross and Filchner–Ronne ice shelves, are quite dependent on the details of the ocean tide models. These models are poorly controlled by actual data at latitudes higher than 65° and are extrapolated using calculations based on rather poor bathymetric models around the Antarctic continent (and hence poorly known water column thicknesses beneath the ice shelves). This suggests in turn that GLAS observations perhaps could be processed to extract the load tides and used to improve ocean tide and bathymetry models in these inaccessible regions.

Conclusions

To achieve geodetic-precision surface elevation measurements over the Antarctic ice sheet (and also over Greenland) by satellite laser altimeter, the measured ranges need to be corrected for ocean-tide loading. These corrections can be calculated conveniently from pre-tabulated amplitudes and phases calculated on a rather coarse (1° x 1°) world-wide grid by simple spatial interpolation. A systematic evaluation of

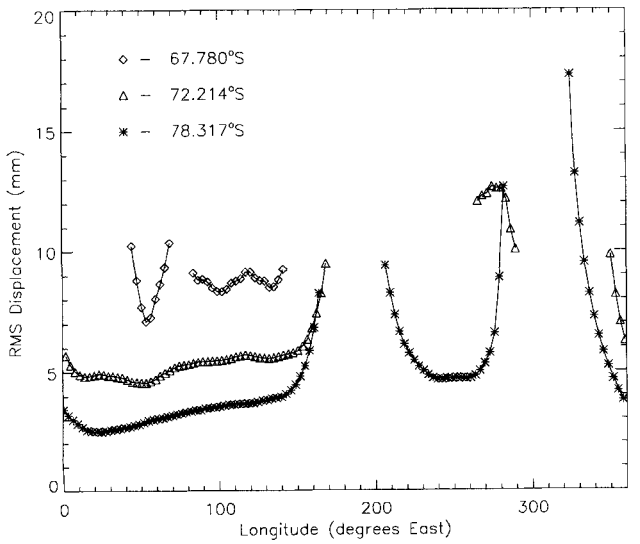


Fig. 5. RMS vertical displacements associated with ocean-tide loading, for crossover points at three latitudes (67.780°S, 72.214°S, and 78.317°S), calculated for the first 45 cycles of ascending and descending passes in the scenario GLAS mission used in Fig. 4. Note the effect of proximity to the coastline.

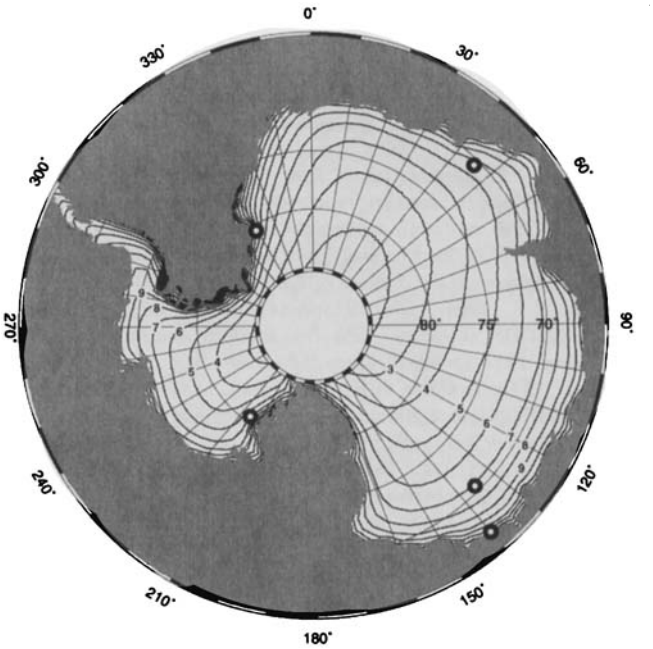


Fig. 6. RMS vertical displacement generated by ocean load tides over the Antarctic continent, during calendar year 2001. Compare with the maximum possible values associated with the same tidal constituents, contoured in Fig. 1. The five locations shown are the same as in Fig. 1.

https://doi.org/10.1017/S0954102000000158 Published online by Cambridge University Press

tidal loading corrections over the Antarctic continent shows that it reaches several centimetres close to the coast line, and averages 10 mm (in an RMS sense) over the entire continent. The oceanic tidal loading correction is particularly important along the coast, which will be a region of special interest for the ICESAT mission because changes are most likely to be found there and because satellite radar altimeters produce poor results on the coastal slopes of the ice sheet.

Acknowledgements

Our thanks to Duncan Agnew for making his software to calculate ocean tide loading available to us and for several illuminating discussions about ocean tide models and load tides. Helen A. Fricker offered detailed comments on the manuscript, which together with constructive reviews from D.E. Cartwright and C. Le Provost improved the text. We also acknowledge interesting exchanges with R. Peltier and J. Wahr concerning load tide calculations by several different methods. B.E. Schutz, GLAS science team leader, provided us with the mission scenario orbit and crossover point calculations. This research was supported by the Geoscience Laser Altimeter System Science Team under Contracts Number NAS5-33019 and NAS5-33015. Contribution No. 579 of the Geophysical and Polar Research Center, University of Wisconsin - Madison.

References

AGNEW, D.C. 1996. SPOTL: Some programs for ocean-tide loading. *Scripps Institution of Oceanography Reference Series*, 96–8, 35 pp.

BAKER, T.F. 1985. Method of tidal loading computation. *Marees Terrestres Bulletin d'Informations*, **94**, 6365–6373.

BENTLEY, C.R. & SHEEHAN, D.D. 1992. Comparison of altimetry profiles over East Antarctic from Seasat and Geosat, an interim report. *Zeitschrift Fur Gletscherkunde und Glazialgeologie*, **26**, 1–9.

BRENNER, A.C., BINDSCHADLER, R.A., THOMAS, R.H. & ZWALLY, H.J. 1983. Slope-induced errors in radar altimetry over continental ice sheets. *Journal of Geophysical Research*, **88**, 1617–1623.

DOODSON, A.T. 1928. The analysis of tidal observations. *Philosophical Transactions Royal Society of London*, **227**, 223–279.

EANES, R.J. 1994. Diurnal and semidiurnal tides from TOPEX/POSEIDON altimetry. *Eos Transactions American Geophysical Union, 1994 Spring Meeting Supplement*, 108.

EGBERT, G.D., BENNETT, A.F. & FOREMAN, M.G.G. 1994. TOPEX/POSEIDON tides estimated using a global inverse model. *Journal of Geophysical Research*, **99**, 24 821–24 852.

FARRELL, W.E. 1972. Deformation of the Earth by surface loads. *Reviews of Geophysics and Space Physics*, **10**, 761–797.

HAINES, B.J., BORN, G.H., WILLIAMSON, R.C. & KOBLINSKY, C.J. 1994. Application of the GEM-T2 gravity field to altimetric satellite orbit computation. *Journal of Geophysical Research*, **99**, 16 237–16 254.

JACOBS, S.S. 1992. Is the Antarctic ice sheet growing? *Nature*, **360**, 29–33.

LE PROVOST, C., GENCO, M.L., LYARD, F., VINCENT, P. & CANCEIL, P. 1994. Spectroscopy of the world ocean tides from a finite element hydrodynamic model. *Journal of Geophysical Research*, **99**, 24 777–24 797.

LE PROVOST, C., BENNETT, A.F. & CARTWRIGHT, D.E. 1995. Ocean tides for and from TOPEX/POSEIDON. *Science*, **267**, 639–642.

LINGLE, C.S., LEE, L., ZWALLY, H.J. & SEISS, T.C. 1994. Recent elevation increase on Lambert Glacier, Antarctic, from orbit crossover analysis of satellite radar altimetry. *Annals of Glaciology*, **20**, 26–32.

MCCARTHY, D.D. *ed.* 1992. IERS Standards. *IERS Technical Note 13*. Paris: Observatoire de Paris.

OERLEMANS, J. 1993. Possible changes in the mass balance of the Greenland and Antarctic ice sheets and their observations, projections and implications. *In* WARRICK, R.A., BARROW, E.M. & WIGLEY, T.M.L., *eds. Climate and sea level change: observations, projections, and implications*. Cambridge: Cambridge University Press, 144–161.

PARKE, M.E., ROBERT, R.H., FARLESS, D.L. & CARTWRIGHT, D.E. 1987. On the choice of orbits for an altimetric satellite to study ocean circulation and tides. *Journal of Geophysical Research*, **92**, 11 693–11 707.

PARTINGTON, K.C., CUDLIP, W. & RAPLEY, C.G. 1991. An assessment of the capability of the satellite radar altimeter for measuring ice sheet topographic change. *International Journal of Remote Sensing*, **12**, 585–609.

PRESS, W.H., TEUKOLSKY, S.A., VETTERLING, W.T. & FLANNERY, B.P. 1992. *Numerical recipes in C*. New York: Cambridge University Press, 994 pp.

RIDLEY, J.K. & PARTINGTON, K.C. 1988. A model of satellite radar altimeter return from ice sheets. *International Journal of Remote Sensing*, **9**, 601–624.

SCHERNECK, H.G. 1991. A parameterized solid earth tide model and ocean tide loading effects for global geodetic baseline measurements. *Geophysical Journal International*, **106**, 677–694.

SCHUTZ, B.E. 1995. Geoscience Laser Altimeter System. *Mission to Planet Earth/Earth Observing System Reference Handbook*, 132–134.

SCHWIDERSKI, E.W. 1988. On charting global ocean tides. *Reviews of Geophysics and Space Physics*, **18**, 243–268.

WARRICK, R.A. 1993. Climate and sea level change: a synthesis *In* WARRICK, R.A., BARROW, E.M. & WIGLEY, T.M.L., *eds. Climate and sea level change: observations, projections, and implications* Cambridge: Cambridge University Press, 3–21.

WARRICK R.A. & OERLEMANS, J. 1990. *Sea level rise. In* HOUGHTON, J.T., JENKINS, G.T. & EPHRAUMS, J.J., *eds. Climate change: the ICPP Scientific Assessment*. Cambridge: Cambridge University Press, 257–281.

YI, D. & BENTLEY, C.R. 1997. A retracking algorithm for satellite radar altimetry over an ice sheet and its applications. *In* COLBECK, S.C., *ed. Glaciers, ice sheets, and volcanoes: A tribute to Mark F. Meier*. U.S. Army Cold Regions Research and Engineering Laboratory, special report 96, **27**, 112–120.

YI, D., BENTLEY, C.R. & STENOIEN, M.D. 1997. Seasonal variation in the height of the East Antarctic ice sheet. *Annals of Glaciology*, **24**, 191–198.

ZWALLY, H.J. 1989. Growth of Greenland ice sheet: interpretation. *Science*, **246**, 1589–1591.

ZWALLY, H.J., BRENNER, A.C., MAJOR, J.A., BINDSCHADLER, R.A. & MARSH, J.G. 1989. Growth of Greenland ice sheet: measurement. *Science*, **246**, 1587–1589.

ZWALLY, H.J., BRENNER, A.C., MAJOR, J.A., MARTIN T.V. & BINDSCHADLER, R.A. 1990. *Satellite radar altimetry over ice. Vol. 1, Processing and corrections of Seasat data over Greenland*. Washington, DC: National Aeronautics and Space Administration.

https://doi.org/10.1017/S0954102000000158 Published online by Cambridge University Press